

# THERMAL STABILITY OF DETF MEMS RESONATORS: NUMERICAL MODELLING AND EXPERIMENTAL VALIDATION

Valentina Zega<sup>1</sup>, Andrea Opreni<sup>1</sup>, Giorgio Mussi<sup>1</sup>, Hyun-Keun Kwon<sup>2</sup>, Gabrielle Vukasin<sup>2</sup>, Gabriele Gattore<sup>3</sup>, Giacomo Langfelder<sup>1</sup>, Attilio Frangi<sup>1</sup> and Thomas W. Kenny<sup>2</sup>

<sup>1</sup>Politecnico di Milano, Milano, ITALY,

<sup>2</sup>Stanford University, Stanford, California, USA, and

<sup>3</sup>STMicroelectronics, Cornaredo, ITALY

## ABSTRACT

The design, fabrication and experimental validation of two MicroElectroMechanical Systems (MEMS) Double-Ended Tuning-Fork (DETF) resonators that exhibit an intrinsic sub-350 ppm thermal stability in the temperature range [5°C – 85°C] are reported.

A strategy for the optimization of the design of MEMS resonators that exhibit high thermal stability and high quality factor is also provided and a good agreement with experimental data is achieved.

The main advantage of the proposed strategy is that it does not require any experimental calibration of the model parameters and can be in principle applied to different kind of resonators, thus representing a powerful tool for the *a-priori* design of thermally stable MEMS resonators with high quality factors.

## KEYWORDS

MEMS, resonators, numerical modelling, thermal stability.

## INTRODUCTION

Real-time clocking applications have been dominated by quartz resonators [1] so far thanks to their good thermal stability (in the order of tens of ppm in the range of temperature [-35°C ; 85°C]), low noise, ageing properties, power handling and high quality factors. Recently, MEMS resonators entered this market as a response to the request of miniaturization and integrability with the electronics and other MEMS devices [2].

To achieve the performances of their quartz counterparts, MEMS resonators must overcome their intrinsic low thermal stability (frequency variation around 3000 ppm in the temperature range [-35°C ; 85°C] for standard polysilicon/single crystal silicon) that mainly depends on the temperature dependence of the elastic constants and of other thermal properties of silicon (thermal expansion coefficient, thermal conductivity, specific heat) and improve their quality factors.

Several solutions have been proposed so far to improve the thermal stability of MEMS resonators. Some examples include, but are not limited to, electronic compensation [3], multi-modal operation of the resonator [4], nonlinear amplitude-frequency coupling and multi-material devices. Furthermore, in [5]-[7] it is shown that for each *n*-doping level of silicon there is an intrinsic minimum in terms of frequency drift in temperature that can be achieved by properly orienting the structure with respect to the crystallographic axes on the wafer. This minimum decreases by increasing the doping level and is independent on the geometric dimensions of the resonator.

On the other side, the quality factor of MEMS resonators is usually dominated by the thermoelastic contribution ( $Q_{TED}$ ) since fluid damping can be considered negligible in vacuum packaged devices and anchor losses are often avoided by design (i.e. tuning fork resonators). In [6],[8] it has been proven that thermoelastic damping can be significantly limited by introducing slots in the deformable arms of the MEMS resonators to reduce heat conduction. In the present paper, we will focus on a classical DETF resonator, fabricated in an *n*-doped single-crystal silicon and vibrating according to an in-plane bending mode. The geometry and the orientation of the DETF on the highly doped single crystal silicon wafer are optimized in order to improve simultaneously the thermal stability and the quality factor of the resonator.

Two DETF resonators (DETF1 and DETF2 in the following) that exhibit an intrinsic sub-350ppm thermal stability are then proposed as the result of two optimization procedures.

## METHOD

Aware of the strong dependence of the thermal stability of MEMS DETF resonators on the doping level of the single crystal silicon, we choose the maximum doping level (Phosphorus  $6.6 \cdot 10^{19} \text{ cm}^{-3}$ ) compatible with the employed fabrication process. From [6], it is known that the best thermal stability achievable for such doping level is a 200 ppm frequency variation in the temperature range of [-35°C ; 85°C].

The geometry of the DETF1 resonator is shown in Figure 1a. The geometric dimensions have been chosen such that the natural frequency of the first in-plane flexural mode (Figure 1b) is in the order of 550 kHz as required by real-time clocking applications. The orientation  $\vartheta$  of the structure on the silicon wafer is then considered in order to maximize the thermal stability of the resonator.

A custom Finite Element Method (FEM) code is employed to compute the natural frequency and the thermoelastic quality factor of the DETF1 under varying temperature conditions [9] and for different orientations  $\vartheta$ . In the code, the temperature dependent material properties of the doped silicon are taken from the literature [10] thus allowing an *a-priori* estimation of the dynamic behavior of the resonator (i.e. no experimental calibration of the model parameters needed). The optimal orientation of the structure with respect to the crystallographic axes is reported in Figure 1a, while the natural frequency and the quality factor at 25°C are reported in the first column of Table I.

In the design process of the DETF1, the thermoelastic quality factor is not taken into account as a parameter to optimize. It is numerically computed by solving the fully

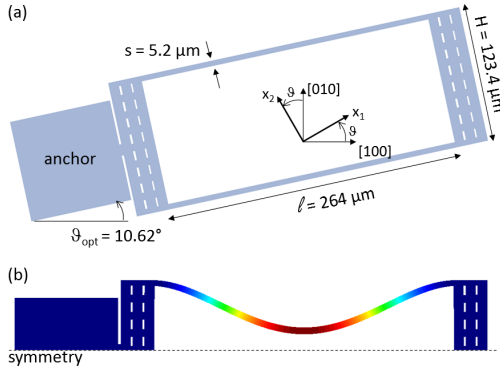


Figure 1: (a) Schematic view of the geometry of the DETF1 resonator. Geometric quantities are reported together with the optimal orientation  $\vartheta_{opt}$  of the device with respect to the crystallographic axes. (b) First flexural mode of the resonator. The contour of the displacement field is reported in color.

coupled thermoelastic problem with zero body forces [11] after the final design of the DETF is obtained. Other sources of damping are neglected as stated in the introduction. They can be added to the FEM model as done in [12] for the fluid contribution and in [13] for anchor losses.

The mechanical design of the DETF2 is instead obtained by simultaneously maximizing the thermal stability and the thermoelastic quality factor through the evolutionary algorithm CMA-ES (Covariance Matrix Adaptation Evolution Strategy) for non-linear, non-convex black-box optimization problems in the continuous domain [14]-[15]. The optimization variables are shown in Figure 2, they describe the geometry of the DETF resonator, the dimensions of the slots on the deformable arms and the orientation  $\theta$  with respect to the [100] crystallographic axis. The multi-objective function reads:

$$f_{obj} = -Q_{TED} + 100 \check{\Delta}f$$

with  $\check{\Delta}f$  defined as:

$$\check{\Delta}f = \frac{\Delta f_0}{f_0(@25^\circ C)} \times 10^6$$

where

$$\Delta f_0 = \max_{T \in [-35^\circ C, +85^\circ C]} f_0(T) - \min_{T \in [-35^\circ C, +85^\circ C]} f_0(T)$$

with  $f_0$  the natural frequency of the in-plane flexural mode of the DETF2 resonator.

The factor of 100 is here introduced to make the two terms of the multi-objective function of the same order of magnitude to facilitate the optimization procedure. As for the DETF1, the desired natural frequency of the in-plane flexural mode must be around 550 kHz. This requirement is considered as a constraint in the optimization procedure together with the fabrication process restrictions (i.e. minimum width of the deformable arms, maximum length of a suspended structure).

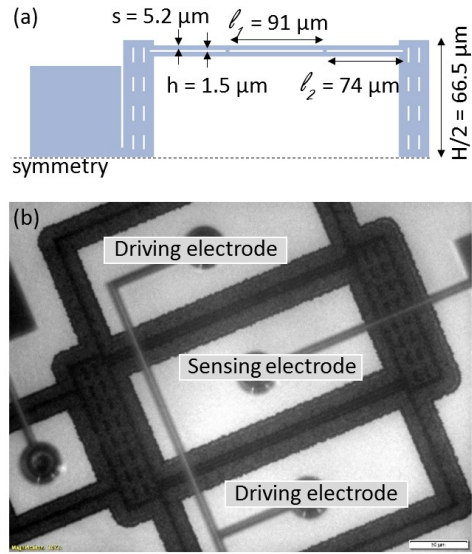


Figure 2: (a) Schematic view of the geometry of the DETF2 resonator. Holes on the flexible arms are added to improve the thermoelastic quality factor. (b) Optic microscope image of the fabricated structure.

Table 1. Comparison between experimental data and numerical results for the DETF1 resonator shown in Figure 1.

	Numerical	Experimental
<b>Natural Frequency</b>	536.8 kHz	477.3 kHz
<b>Quality factor [-]</b>	45318	31379
<b><math>\Delta f</math> @ [5°C – 85°C]</b>	200 ppm	190 ppm

Table 2. Comparison between experimental data and numerical results for the DETF2 resonator shown in Figure 2.

	Numerical	Experimental
<b>Natural Frequency</b>	550.8 kHz	472.4 kHz
<b>Quality factor [-]</b>	96463	66796
<b><math>\Delta f</math> @ [5°C – 85°C]</b>	200 ppm	350 ppm

The optimization results show that it is possible to increase the quality factor by a factor of 2 (see first column of Table 2) by maintaining all other properties unchanged only by modifying the geometry of the device (e.g. holes are added on the deformable arms).

The optimal orientation of the structure with respect to the crystallographic axis [100] is  $\theta_{opt} = 9.54^\circ$  and it allows a frequency variation of 200 ppm in the temperature range of [-35°C ; 85°C] as expected. It is worth stressing that the choice made on the optimization variables (i.e. number of slots in the deformable arm of the DETF resonator) influence the final results. A higher quality factor can in

principle be achieved by increasing the number of the slots in the in-plane thickness of the arms of the DETF resonator. Other optimization variables can be also added according to the needs of the MEMS resonator designer thus proving the generality of the proposed design strategy.

## EXPERIMENTAL RESULTS

The two DETF resonators have been fabricated through the epi-seal encapsulation process proposed by researchers at the Robert Bosch Research and Technology Center in Palo Alto and then demonstrated with Stanford University.

As shown in the optical microscope image in Figure 2b, two electrodes are located on the external sides of the flexible arms of the DETF resonator to provide the electrostatic actuation (i.e. Alternating Current (AC) voltage), while one electrode is located between the two arms to allow the readout. A nominal gap of 1.5  $\mu\text{m}$  is present between the electrodes and the arms of the DETF resonator is present.

A first experimental characterization of the devices in terms of natural frequency and quality factor, carried out with a custom transimpedance amplifier and a HP4195A network analyzer, shows a satisfactory agreement between experimental data and numerical predictions (Tables 1-2). The predicted increase of the thermoelastic quality factor of the DETF2 with respect to the DETF1 resonator and the high thermal stabilities of the two devices are confirmed by experiments.

The discrepancies in terms of natural frequencies and quality factor can be mainly ascribed to the uncertainties related to the fabrication process (e.g. doping level of the silicon, material properties, over etch and other fabrication imperfections) and to the assumption that all the sources of damping are negligible except for the thermoelastic one.

Finally, the measurement of the frequency variation in temperature of the two DETF resonators is obtained by placing the devices in a custom electronic oscillator inside a climatic chamber and measuring the resulting oscillation through a frequency meter.

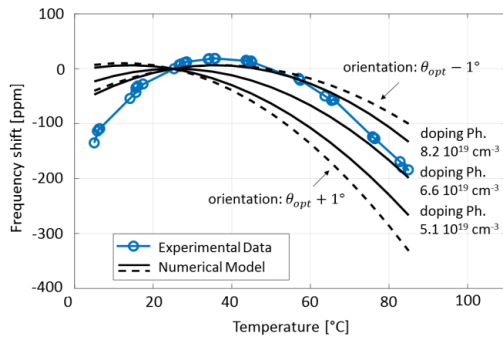


Figure 3: Frequency variation in temperature (defined as  $(f(T)-f(25^\circ\text{C}))/f(25^\circ\text{C}) \cdot 10^6$ ) for the DETF1 resonator shown in Figure 1a. Experimental data are compared to numerical predictions computed for three different phosphorus doping levels (solid lines) and for three different orientations of the structure on the silicon wafer (dotted lines).

In Figure 3, the experimental results in terms of frequency variation in temperature obtained for the DETF1 are compared with numerical predictions computed through the above mentioned custom FEM code.

The agreement between experimental data (blue line in Figure 3) and numerical model with nominal parameters is overall good, but shows some discrepancies as expected from Tables 1-2.

Uncertainties on the doping level and on the orientation of the silicon wafer are then taken into account: the doping level and the orientation tolerance with respect to the nominal ones are spanned within an admissible range provided by the fabrication process.

Uncertainties coming from the experimental set-up (i.e. stability of the climatic chamber especially for negative temperatures) should be also considered for a quantitative comparison between experimental and numerical curves.

In Figure 4, the frequency variation induced by temperature fluctuations measured on two different prototypes of the DETF2 resonator (blue and orange lines in Figure 4) are reported together with the numerical predictions computed for three different levels of doping: the nominal one, the maximum and minimum admissible for the employed fabrication process. The small discrepancy between the two experimental curves can be ascribed to fabrication imperfections (i.e. over etch).

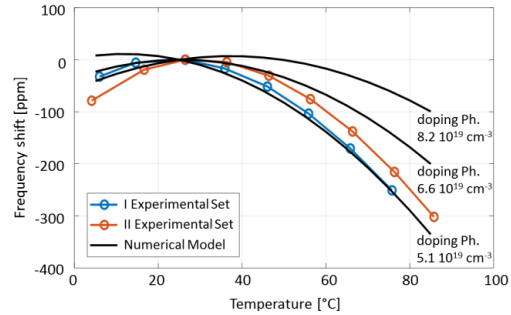


Figure 4: Frequency variation in temperature for the DETF2 resonator shown in Figure 2. Experimental data (two devices) are compared to numerical predictions computed for three different phosphorus doping levels of the silicon wafer.

## CONCLUSIONS

Two MEMS DETF resonators have been designed, fabricated and experimentally tested.

The devices are fabricated in highly doped single crystal silicon that allow for an intrinsic thermal stability of a 200 ppm frequency variation in a temperature range of  $[-35^\circ\text{C}; 85^\circ\text{C}]$  for a specific orientation of the resonator with respect to the crystallographic axes.

The mechanical design of the two proposed devices comes from optimization procedures properly developed by the authors. Geometric dimensions and the orientation of the structure on the silicon wafer are chosen as optimization variables, while the objective function are the frequency variation in temperature (DETF1) or its combination with the thermoelastic quality factor (DETF2).

It is shown that it is possible to double the quality factor by

playing with the geometry of the resonator without sacrificing thermal stability.

All the simulations are performed *a-priori*, by considering nominal dimensions of the DETF resonator and material properties available in the literature, thus providing generality to the proposed strategy.

Moreover, it is possible to introduce other optimization variables or to change the (multi-)objective function or the constraints in the proposed procedure according to the needs of the MEMS resonators designer.

The proposed design strategy can in principle be applied to different kinds of MEMS resonators (e.g. Lamè, torsional, extensional) since it is not an ad-hoc procedure for DETF resonators.

The agreement between the experiments and the predicted frequency variation in temperature is good. A better quantitative agreement can be achieved by improving the experimental set-up and/or by characterizing the material properties of the employed highly doped single crystal silicon through ad-hoc structures instead of using material properties coming from the literature and referred to different processes or different wafers.

We are currently working on the characterization of the material properties in temperature through the design, fabrication and testing of structures properly designed to measure the alignment of the crystallographic axes with the nominal directions [100] and [010], the thermal conductivity, the thermal expansion coefficient and thermal capacitance.

## REFERENCES

- [1] O Nizhnik, K Higuchi, K Maenaka, 'Quartz Resonator Based, 0.12  $\mu$ W, 32768 Hz Oscillator with  $\pm 100$  ppm Frequency Accuracy', *J. Low Power Electron. Appl.* 2011, 1(2), (2011), pp. 327-333.
- [2] SiTime. SiT1532 Ultra-Small 32 kHz Oscillator. Available online: [www.sitime.com](http://www.sitime.com) (accessed on 9 June 2018).
- [3] S A G Zadeh, T Saha, K Allidina, K Nabki, M N El-Gamal, 'Electronic temperature compensation of clamped-clamped beam MEMS resonators', *Proc. 53<sup>rd</sup> IEEE Int. Midwest Symp. On Circuits and Systems* 2010, pp. 1193-1196.
- [4] H-K Kwon, L C Ortiz, G D Vukasin, Y Chen, D D Shin, T W Kenny, 'An oven-controlled MEMS oscillator (OCMO) with sub 10MW,  $\pm 1.5$  ppb stability over temperature', *Proc. Transducers 2019-Eurosensors XXXIII*, pp. 2072-2075.
- [5] A Jaakkola, M Prunnila, T Pensala, J Dekker, P Pekko, 'Design rules for temperature compensated degenerately n-type doped silicon MEMS resonators', *J. Microelectromech. Syst.*, 24 (2015), pp. 1832-1839.
- [6] V Zega, A Frangi, A Guercilena, G Gattere, 'Analysis on thermal stability and thermoelastic effects for slotted tuning fork MEMS resonators', *Sensors*, 18 (2018), pp. 2157.
- [7] E J Ng, V A Hong, Y Yang, C H Ahn, C L M Everhart, T W Kenny, 'Temperature dependence of the elastic constants of doped silicon', *J. MicroElectromech. Syst.*, 24, (2015) pp. 730-741.
- [8] R N Candler, A Duwel, M Varghese, S A Chandorkar, M A Hopcroft, W-T Park, B Kim, G Yama, A Partridge, M Lutz, et al. 'Impact of geometry on thermoelastic dissipation in micromechanical resonant beams', *J. MicroElectromech. Syst.*, 15, (2006), pp. 927-934.
- [9] B Kim, M A Hopcroft, R N Candler, C M Jha, M Agarwal, R Melamud, S A Chandorkar, G Yama, T W Kenny, 'Temperature dependence of quality factor in MEMS resonators', *J. Microelectromech. Syst.* 17, (2008), pp. 755-766.
- [10] A Jakkola, M Prunnila, T Pensala, J Dekker, P Pekko, 'Determination of doping and temperature dependent elastic constants of degenerately doped silicon from MEMS resonators' *Proc. IEEE Trans. Ultrason. Ferroelectr. Freq. Control* 2014, 61, pp. 1063-1074.
- [11] A Corigliano, R Ardito, C Comi, A Frangi, A Ghisi, S Mariani, 'Mechanics of Microsystems', Wiley: Hoboken, NJ, USA, (2018).
- [12] P Fedeli, A Frangi, G Laghi, G Langfelder, G Gattere, 'Near vacuum gas damping in MEMS: Simplified modeling', *J. Microelectromech. Syst.*, 26, (2017), pp. 632-642.
- [13] A Frangi, M Cremonesi, 'Semi-analytical and numerical estimates of anchor losses in bistable MEMS', *Int. J. Solids Struct.*, 92-93, (2006), pp. 141-148.
- [14] N Hansen, S D Müller, P Koumoutsakos, 'Reducing the Time Complexity of the Derandomized Evolution Strategy with Covariance Matrix Adaptation (CMA-ES)', *Evol. Comput.* 11, (2003), pp. 1-18.
- [15] N Hansen, A Ostermeier, 'Completely Derandomized Self-Adaptation in Evolution Strategies', *Evol. Comput.* 9, (2001), pp. 159-195.

## CONTACT

\*V. Zega, tel: +39-0223996312;  
valentina.zega@polimi.it